ZnO Nanostructures

Single-Crystal Hexagonal Disks and Rings of ZnO: Low-Temperature, Large-Scale Synthesis and Growth Mechanism**

Feng Li, Yong Ding, Puxian Gao, Xinquan Xin, and Zhong L. Wang**

The optical response of a particle depends on its particular size, shape, and local dielectric environment.[1] Synthesis of size- and shape-controlled nanostructures is important in controlling their chemical and physical properties.[2,3] ZnO, with a wide band gap of 3.37 eV, is a candidate for

[*] Dr. F. Li
Department of Chemistry
University of New Orleans
New Orleans, LA 70148 (USA)
Fax: (+1) 504-280-6860
E-mail: fli@uno.edu
Dr. Y. Ding, P. Gao, Prof. Dr. Z. L. Wang
School of Materials Science and Engineering
Georgia Institute of Technology
Atlanta, GA 30332-0245 (USA)
Fax: (+1) 404-894-9140
E-mail: zhong.wang@mse.gatech.edu
Prof. X. Xin
Department of Chemistry
Nanjing University
Nanjing 20093 (P. R. China)

[**] The authors gratefully acknowledge the financial support of the National Science Foundation of China (No.90101028) and the National Science Foundation.

  DOI: 10.1002/ange.200460783

applications in electronics, photoelectronics, and sensors.[4–9] Among the developed approaches, solid–vapor phase growth (SVG) at high temperature is favored for its simplicity and high-quality in producing ZnO nanowires, nanobelts, nanocantilevers, and nanonails.[6–17] In addition to fabrication of rings by lithography[1,18–20] and self-assembly[21,22], our recent significant progress based on the SVG approach is the synthesis of single-crystal ZnO rings from self-assembled polar nanobelts.[23,24] The SVG approach has been used for discovering a diversity of nanostructures,[25] but its major limitation is low yield.

Solution phase synthesis (SPS), including microemulsion and hydrothermal growth, has also proved effective and convenient in preparing ZnO nanowires, nanorods, and helical rods at low temperature on a large scale.[4,5,26–32] In this approach, it is believed that the shape of micelles plays a key role in the controlled growth of one-dimensional (1D) nanostructures in solution.[26] Since surfactants can be made to form micelles with diverse shapes from spheres to rods to ellipsoids to disks, and even much more complex shapes, by adjusting experimental parameters,[33] we can further control the nanostructures by means of the SPS approach. Here we report a rational synthesis of single-crystal hexagonal ZnO nanodiscs and rings on a large scale by the SPS approach, and demonstrate its potential for low-temperature, large-scale, controlled synthesis of single-crystal ZnO nanostructures. The approach may be extendible to the synthesis of a wide range of nanomaterials. The hexagonal disks and rings are new members in the family of ZnO nanostructures. On the basis of structural information provided by electron microscopy, a growth mechanism is proposed for the formation of disks and rings.

The ZnO rings and disks were synthesized by a solution-phase approach. The procedure involves 1) preparation of an oil-in-water microemulsion with surfactant, namely, sodium bis(2-ethylhexyl) sulfosuccinate (NaAOT), in a water/1-butanol/$Zn(NO_3)_2$ system, and 2) subsequent growth of ZnO rings and disks in microreactors. Figure 1a shows a typical low-magnification SEM image of ZnO nanostructures grown at 70 °C. The as-synthesized product is pure and uniform, and is dominated by hexagonal-based thin disks with uniform size and well-defined shape. The disks are 2–3 μm in diameter and 50–200 nm thick. An enlarged image shows the back-to-back paired stacking of the disks (Figure 1b), with one side of the disk surface smoother, and the other rougher. The two adjacent contacting surfaces are rather smooth. Some of the disks have a hole at the middle, and are thus hexagonal rings (Figure 1c).

The morphology of the disks can be modified by adjusting the growth temperature. Increasing the growth temperature from 70 to 90 °C dramatically increases the yield of hexagonal rings (Figure 2a). Most of the rings have a hexagonal base and their morphology is fairly uniform. The size of the inner holes varies from ring to ring, and they are mostly hexagonal (Figure 2b, c). In some cases, the shape of the hole is irregular (Figure 2d).

Detailed examination revealed that the top and bottom surfaces of the hexagonal rings and disks are quite different; one side is smooth, and the other rough (Figure 3a). The rough side had a higher "etching" rate (see below), so that the surface is nonuniform, and there is a small hole at the middle (Figure 3b). The nonuniform morphology of the top surface can be best seen by tilting the disk (Figure 3c), which reveals the grooved surface structure associated with the crystal symmetry on one side (Figure 3d). In contrast, the backside of the ring is rather flat. The hole appeared to have been created from the rougher side and extends half way through the thickness (Figure 3e). For a small hole that passes throughout

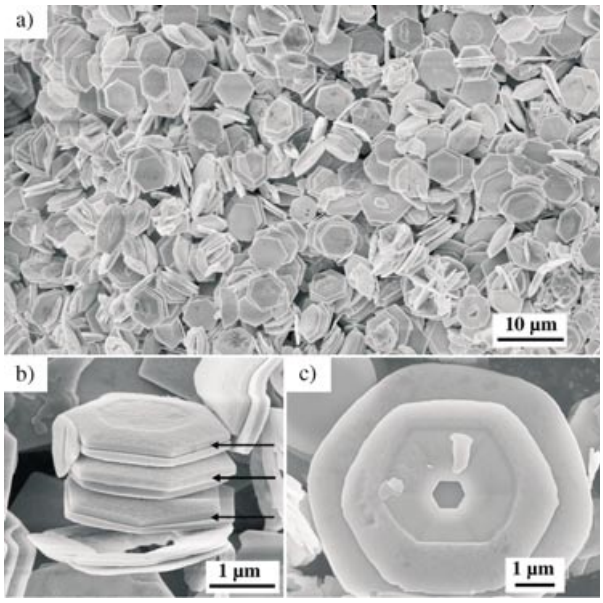

Figure 1. a) Low-magnification SEM image recorded from the as-synthesized ZnO sample prepared at 70 °C, demonstrating the predominance of hexagonal disks. b), c) Enlarged SEM images displaying detailed structures of the hexagonal disks.

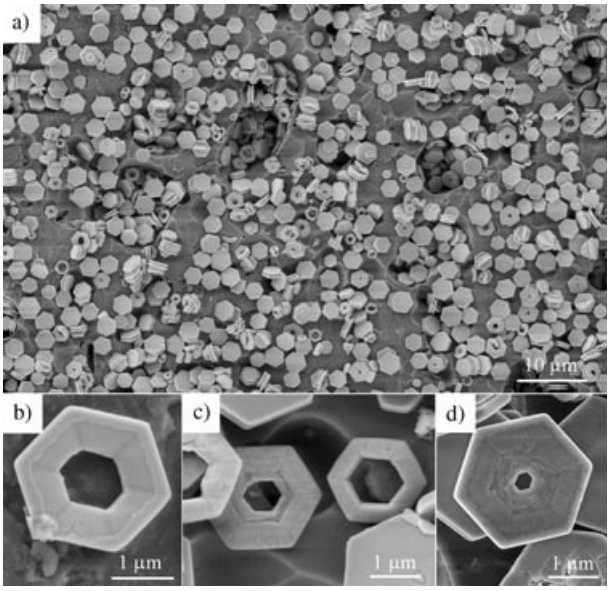

Figure 2. a) Low-magnification SEM image recorded from the as-synthesized ZnO sample prepared at 90 °C; the higher yield of hexagonal rings is evident. b)–d) Enlarged SEM images displaying detailed structures of the hexagonal rings.

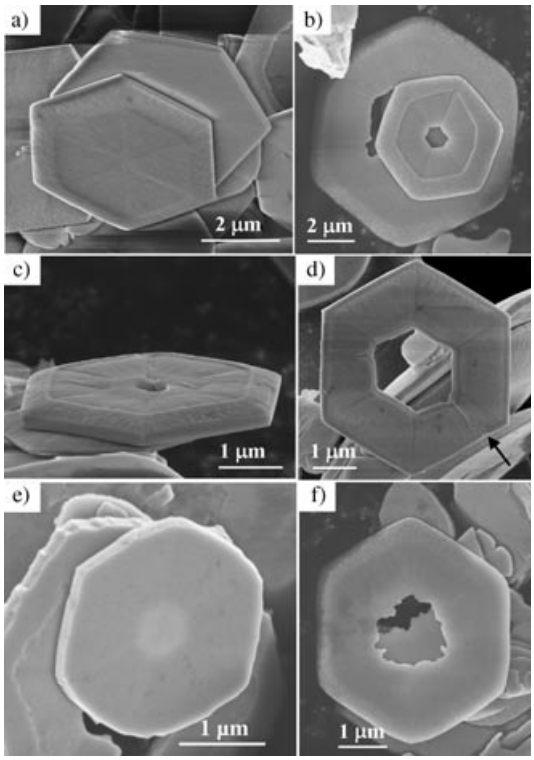

Figure 3. SEM images recorded from ZnO hexagonal disks showing the structural features on the rougher and smoother surfaces of the disks.

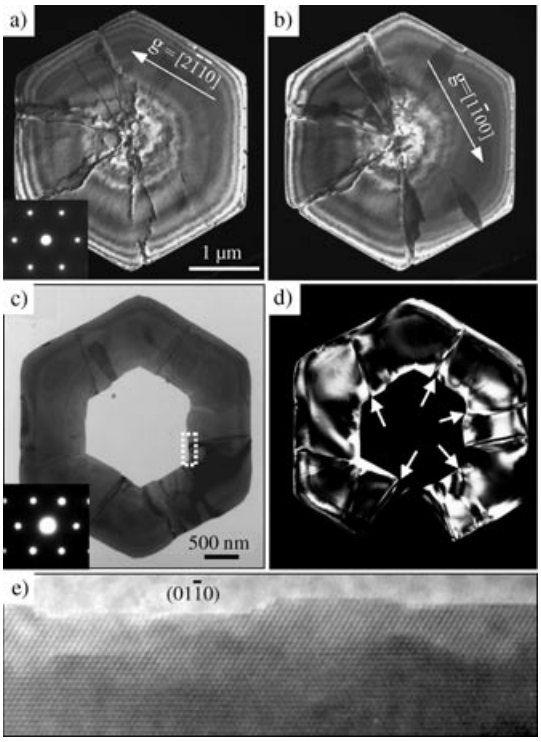

Figure 4. a), b) Dark-field TEM images and corresponding diffraction pattern of a hexagonal disk, showing planar defects in the disk, which are likely to be low-angle grain boundaries induced during crystal growth. c) Bright-field TEM image of a hexagonal ring and its corresponding diffraction pattern, showing that the ring has a top/bottom (0001) surfaces and inner/outer {1$\bar{1}$00} surfaces. d) Dark-field TEM image of the ring, displaying defects closely parallel to {2$\bar{1}\bar{1}$0}. e) High-resolution TEM image recorded from the inner edge marked in c), showing clean and sharp surfaces.

the thickness, a rough edge at the inner surface is apparent (Figure 3 f).

The TEM analysis of the hexagonal disk showed a single-crystal structure, with (0001) top/bottom surfaces, and {1$\bar{1}$00} side facets (Figure 4 a). The dark-field image of the disk shows defects, which are distributed radially with a higher concentration at the center. The defects are most likely low-angle grain boundaries (Figure 4 b). Some thickness fringes are observed, which correspond to the reduced thickness towards the center.

The hexagonal ring also shows a single-crystal structure, with (0001) top/bottom surfaces and {1$\bar{1}$00} side surfaces (Figure 4 c, d). An important feature observed in the TEM image is the presence of defects closely parallel to ⟨2$\bar{1}\bar{1}$0⟩ in the ring. The disk has a wedge shape that becomes thinner towards the center. A high-resolution TEM image recorded from the inner edge of the ring (Figure 4 e) shows surface steps, atomically sharp and free of contamination. The TEM image also reveals the decrease in disk thickness towards the center.

Several experiments were carried out to determine the parameters other than temperature that are important for the formation of disks and rings: 1) No hexagonal ZnO disks were produced in the absence of NaAOT or when NaAOT was replaced with sodium dodecyl sulfate (SDS). 2) The use of *n*-butanol is also crucial to the formation of shape-controlled ZnO disks. No hexagonal ZnO disks are produced in the reaction if only water is used as solvent to dissolve NaAOT, or *n*-butanol is replaced with octane. 3) Zn^{2+} cations can react with AOT^- directly to form white precipitates in water. 4) Further investigations revealed that the molar ratio of Zn^{2+} to $NH_3{\cdot}H_2O$ is one of the dominant parameters for the formation of well-structured disks and rings. Hexagonal disks and rings are produced at $Zn^{2+}/NH_3{\cdot}H_2O$ molar ratios of $^1/_3$, $^1/_4$, $^1/_5$, and $^1/_6$, but no ZnO particles were observed in a reaction carried out at a molar ratio of $^1/_2$. Thus, in the oil-in-water microemulsion system, the reaction temperature and the concentration of $NH_3{\cdot}H_2O$ are the dominant parameters in the formation of hexagonal rings and disks.

On the basis of the information we have gathered, a growth process of the hexagonal disks and rings can be proposed. From the crystal structure, ZnO can be described as a number of alternating planes composed of tetrahedrally coordinated O^{2-} and Zn^{2+} ions, stacked alternatingly along the *c* axis. The oppositely charged ions produce positively charged Zn^{2+} (0001) and negatively charged O^{2-} (000$\bar{1}$) polar surfaces. Therefore, the positively charged Zn^{2+} (0001) and the negatively charged O^{2-} (000$\bar{1}$) surfaces can have very different self-catalysis properties,[11] and the spontaneous polarization along the *c* axis leads to the formation of nanosprings,[24] rings,[23] and nanobows[26] due to electrostatic interaction. The large polar surface is generally energetically unfavorable unless the surface charge is compensated by a passivation agent. On the other hand, it was reported that the

anionic surfactant NaAOT can be made to form micelles with diverse shapes by adjusting experimental parameters.[33–36] The self-assembled AOT^- layers at the interface of water and oil could act as template for growing ZnO. The hydrophilic head of AOT^- can form an anionic surface exposed to water, and thus Zn^{2+} cations can directly attach to the negatively charged AOT^- template to initiate the first layer of crystal growth [Eq. (1)]. The produced $Zn(AOT)_2$ then can be transformed into $[Zn(NH_3)_4]^{2+}$ by reaction with $NH_3{\cdot}H_2O$ [Eq. (2)], so that the positively charged Zn^{2+} (0001) surface of ZnO tends to directly interface with the anionic surface of the AOT^- template in the subsequent hydration of $[Zn(NH_3)_4]^{2+}$ at higher temperature [Eq. (3)].[29]

$$Zn(NO_3)_2\ (aq) + 2\,NaAOT \rightarrow Zn(AOT)_2\ (s) + 2\,NaNO_3\ (aq) \quad (1)$$

$$Zn(AOT)_2\ (s) + 4\,NH_3 \cdot H_2O\ (aq) \rightarrow [Zn(NH_3)_4]^{2+}\ (aq) + 2\,AOT^-\ (aq) + 4\,H_2O\ (l) \quad (2)$$

$$[Zn(NH_3)_4]^{2+}\ (aq) + 3\,H_2O\ (l) \rightleftharpoons ZnO\ (s) + 2\,NH_4^+\ (aq) + 2\,NH_3 \cdot H_2O\ (aq) \quad (3)$$

Fast growth along $\langle 2\bar{1}\bar{1}0\rangle$ results in the formation of a hexagonal disk (Figure 5a). Slight bending of the self-assembled AOT^- monolayer makes it possible to accommodate local strain in the disk by formation of small-angle grain

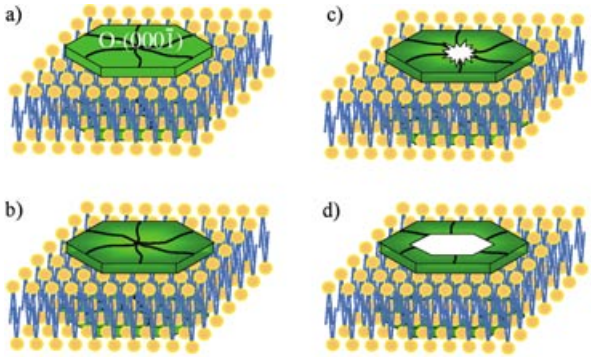

Figure 5. Proposed formation process of the ZnO hexagonal disks and rings, as well as their back-to-back stacking.

boundaries closely parallel to $\{2\bar{1}\bar{1}0\}$. Therefore, some of the grown disks may have this defect.

The Zn^{2+} (0001) surface bonds strongly to AOT^- due to charge interaction, and the densely packed AOT^- will protect the surface from further "etching" or reaction, resulting in the formation of the flat side of the disks (see Figures 1 and 3). The AOT^- template stabilizes the surface charge and the structure.

The exposed negatively charged O^{2-} $(000\bar{1})$ surface of the disk may be reactive towards NH_4^+ and $NH_3{\cdot}H_2O$, as shown in Equation (3). The equilibrium will move in the reverse direction on adding excess $NH_3{\cdot}H_2O$. The rate toward the reverse direction of Equation (3) also increases drastically with increasing temperature; thus, etching of the O^{2-} $(000\bar{1})$ surface by NH_4^+ and excess NH_3 results in the rougher surface (see Figure 3a).

From the TEM image presented in Figure 4b, the density of defects is highest at the center of the disk. A higher etching/reaction rate is possible at the defect sites. Therefore, a high density of planar defects at the center may result in a higher local etching rate and eventually lead to the formation of a hole at the center. The hole is initiated from the O^{2-} $(000\bar{1})$ surface and it may not penetrate the entire thickness if the reaction time is insufficient (see Figure 3e), as presented in Figure 5b. As the reaction proceeds, the etching can create a hole through the disk (Figure 5c). As the hole becomes larger, its side surfaces eventually take on the lower energy $\{1\bar{1}00\}$ facets of ZnO, and the disk becomes a hexagonal ring (Figure 5d). The grooved feature on the surface of the ring along $\langle 2\bar{1}\bar{1}0\rangle$ may be due to the dependence of the local etching rate on the crystal orientation. On the other hand, the etching rate is sensitive to the growth temperature and the molar ratio of reactants; thus rings were not formed at 70 °C, but at 90 °C or higher.

The formation of paired disks, as seen in Figure 1b, may be due to the fact that AOT^- usually forms self-assembled double layers and multilayers in lamellar micelles. The growth of ZnO disks and rings can take place simultaneously on both sides of the template and thus result in back-to-back growth of paired disks or rings. After removing the oil phase from the system, a close attachment of the two disks at the smoother surfaces is energetically favorable because of the van der Waals interaction between the long tails of the self-assembled AOT^- monolayer on the surfaces.

In summary, using NaAOT as template, we have demonstrated a solution-based synthesis of ZnO rings and disks at low temperature and on a large scale. The as-synthesized materials are structurally uniform and pure. By controlling growth temperature and molar ratio of reactants, the disks could converted into rings. The growth mechanism of the hexagonal disks is suggested to be due to charge compensation of the anionic AOT^- template at the Zn^{2+} (0001) surface of ZnO; fast growth along $\langle 2\bar{1}\bar{1}0\rangle$ forms hexagonal disks enclosed by $\{10\bar{1}0\}$ facets. A higher density of defects at the center of the disk results in a higher local reaction/etching rate by NH_4^+ and NH_3. A through-thickness hole, as defined by the $\{10\bar{1}0\}$ facets at the center, leads to the formation of a hexagonal ring. The technique demonstrated here could be extended for synthesizing a wide range of nanomaterials. Using such well-structured materials as building blocks, one could design a diverse range of nanodevices, from nanoscale lasers to sensors and photonic crystals.

Experimental Section

For the preparation of ZnO discs and rings, a NaAOT microemulsion was first prepared by adding an aqueous solution of $Zn(NO_3)_2{\cdot}6\,H_2O$ (0.025 M) to a solution of NaAOT (0.10 M) in 1-butanol and vigorously stirring for 2 h. The volume ratio of the aqueous phase to the organic phase was 10:1. Then a concentrated aqueous solution of $NH_3{\cdot}H_2O$ (17.65 M) with 4:1 molar ratio to $Zn(NO_3)_2{\cdot}6\,H_2O$ was added dropwise to the well-stirred microemulsion. After addition was complete, stirring was continued for 3 h at room temperature. The resulting milky white mixture was subsequently kept at 70 or 90 °C for 5 days. A white suspension was obtained and centrifuged to separate the precipitate, which was washed several times with distilled water and

absolute ethanol. Finally, a white powder was obtained by drying at 70 °C in vacuum. The as-synthesized samples were first analyzed with a LEO 1530 field-emission scanning electron microscope (FE-SEM). Transmission electron microscopy was carried out at 400 kV with a JEOL 4000EX.

Received: May 25, 2004

Keywords: crystal growth · nanostructures · oxides · zinc

[1] J. Aizpurua, P. Hanarp, D. S. Sutherland, M. Käll, G. W. Bryant, F. J. García de Abajo, *Phys. Rev. Lett.* **2003**, *90*, 57401.
[2] F. Li, J. He, W. Zhou, J. B. Wiley, *J. Am. Chem. Soc.* **2003**, *125*, 16166.
[3] F. Li, L. Xu, W. L. Zhou, J. He, R. H. Baughman, A. A. Zakhidov, J. B. Wiley, *Adv. Mater.* **2002**, *14*, 1528.
[4] K.-S. Choi, H. C. Lichtenegger, G. D. Stucky, E. W. McFariand, *J. Am. Chem. Soc.* **2002**, *124*, 12402.
[5] J. Zhang, L. Sun, J. Yin, H. Su, C. Liao, C. Yan, *Chem. Mater.* **2002**, *14*, 4172.
[6] P. X. Gao, Z. L. Wang, *J. Am. Chem. Soc.* **2003**, *125*, 11299.
[7] X. D. Wang, C. J. Summers, Z. L. Wang, *Nano Lett.* **2004**, *4*, 423.
[8] J. Q. Hu, Y. Bando, J. H. Zhan, Y. B. Li, T. Sekiguchi, *Appl. Phys. Lett.* **2003**, *83*, 4414.
[9] J. Y. Lao, J. G. Wen, Z. F. Ren, *Nano Lett.* **2002**, *2*, 1287.
[10] M. H. Huang, S. Mao, H. Feick, H. Yan, Y. Wu, H. Kind, E. Weber, R. Russo, P. Yang, *Science* **2001**, *292*, 1897.
[11] Z. L. Wang, X. Y. Kong, J. M. Zuo, *Phys. Rev. Lett.* **2003**, *91*, 185502.
[12] H. Yan, R. He, J. Johnson, M. Law, R. J. Saykally, P. Yang, *J. Am. Chem. Soc.* **2003**, *125*, 4728.
[13] W. I. Park, G.-C. Yi, M. Kim, S. J. Pennycook, *Adv. Mater.* **2002**, *14*, 1841.
[14] Z. W. Pan, Z. R. Dai, Z. L. Wang, *Science* **2001**, *291*, 1947.
[15] P. X. Gao, Z. L. Wang, *J. Phys. Chem.* **2002**, *106*, 12653.
[16] J.-J. Wu, S.-C. Liu, *Adv. Mater.* **2002**, *14*, 215.
[17] P. Hu, Y. Liu, X. Wang, L. Fu, D. Zhu, *Chem. Commun.* **2003**, 1304.
[18] N. Jiang, G. G. Hembree, J. C. H. Spence, J. Qin, F. J. García de Abajo, J. Silcox, *Appl. Phys. Lett.* **2003**, *83*, 551.
[19] M. Mayer, M. Korkusinski, P. Hawrylak, T. Gutbrod, M. Michel, A. Forchel, *Phys. Rev. Lett.* **2003**, *90*, 186801.
[20] H. Xu, W. A. Goedel, *Angew. Chem.* **2003**, *42*, 4845; *Angew. Chem. Int. Ed.* **2003**, *42*, 4696.
[21] K. T. Nam, B. R. Peelle, S.-W. Lee, A. M. Belecher, *Nano Lett.* **2004**, *4*, 23.
[22] W. L. Zhou, J. He, J. Fang, T.-A. Huynh, T. J. Kennedy, K. L. Stokes, C. J. O'Connor, *J. Appl. Phys.* **2003**, *93*, 7340.
[23] X. Y. Kong, Y. Ding, R. Yang, Z. L. Wang, *Science* **2004**, *303*, 1348.
[24] X. Y. Kong, Z. L. Wang, *Nano Lett.* **2003**, *3*, 1625.
[25] Z. L. Wang, *Mater. Today* **2004**, *7*(6), 26.
[26] W. Hughes, Z. L. Wang, *J. Am. Chem. Soc.* **2004**, *126*, 6703.
[27] L. Guo, Y. L. Ji, H. Xu, P. Simon, Z. Wu, *J. Am. Chem. Soc.* **2002**, *124*, 14864.
[28] Z. R. Tian, J. A. Voigt, J. Liu, B. Mckenzie, M. J. Mcdermott, M. A. Rodriguez, H. Konishi, H. Xu, *Nat. Mater.* **2003**, *2*, 821.
[29] C. Pacholski, A. Kornowski, H. Weller, *Angew. Chem.* **2002**, *114*, 1234–1237; *Angew. Chem. Int. Ed.* **2002**, *41*, 1188–1191.
[30] Z. Li, Y. Xie, Y. Xiong, R. Zhang, W. He, *Chem. Lett.* **2003**, *32*, 760.
[31] Z. R. Tian, J. A. Voigt, J. Liu, B. Mckenzie, M. J. Mcdermott, *J. Am. Chem. Soc.* **2002**, *124*, 12954.
[32] B. Liu, H. C. Zeng, *J. Am. Chem. Soc.* **2003**, *125*, 4430.
[33] L. E. Greene, M. Law, J. Goldberger, F. Kim, J. C. Johnson, Y. Zhang, R. J. Saykally, P. Yang, *Angew. Chem.* **2003**, *115*, 3139; *Angew. Chem. Int. Ed.* **2003**, *42*, 3031.
[34] M. Magalhães, D. Pusiol, M. E. Rania, A. M. Figueiredo Nedo, *J. Chem. Phys.* **1998**, *108*, 3835.
[35] A. I. Bulavchenko, A. F. Batishchev, E. K. Batishcheva, V. G. Torgov, *J. Phys. Chem.* **2002**, *106*, 6381.
[36] R. Köhling, J. Woenckhaus, N. L. Klyachko, R. Winter, *Langmuir* **2002**, *18*, 8626.

